Atom-Photon Spin-Exchange Collisions Mediated by Rydberg Dressing

Fan Yang,[1] Yong-Chun Liu,[1,2,*] and Li You[1,2,3,†]
[1]State Key Laboratory of Low Dimensional Quantum Physics, Department of Physics, Tsinghua University, Beijing 100084, China
[2]Frontier Science Center for Quantum Information, Beijing 100084, China
[3]Beijing Academy of Quantum Information Sciences, Beijing 100193, China

(Received 29 January 2020; accepted 18 August 2020; published 28 September 2020)

We show that a single photon propagating through a Rydberg-dressed atomic ensemble can exchange its spin state with a single atom. Such a spin-exchange collision exhibits both dissipative and coherent features, depending on the interaction strength. For strong interaction, the collision dissipatively drives the system into an entangled dark state of the photon with an atom. In the weak interaction regime, the scattering coherently flips the spin of a single photon in the multiphoton input pulse, demonstrating a generic single-photon subtracting process. An analytical treatment of this process reveals a universal trade-off between efficiency and purity of the extracted photon, which applies to a wide class of single-photon subtractors. We show that such a trade-off can be optimized by adjusting the scattering rate under a novel phase-matching condition.

DOI: 10.1103/PhysRevLett.125.143601

Achieving strong light-atom interactions at the single-particle level represents a long-standing goal in quantum optics [1]. Realizing this goal will not only enable one to test fundamental physics in quantum electrodynamics (QED) [2–6], but it will also facilitate meaningful applications of quantum communication [7–9], simulation [10–13], and metrology [14–16]. As a promising approach, interfacing photons with Rydberg atoms [17] via electromagnetically induced transparency (EIT) [18] has attracted much attention in recent years [19–31]. To date, a host of interaction processes have been established with this approach, e.g., a single atomic excitation can block the transmission of a single photon [19–23], imprint a global phase onto a single photon [25–27], reflect a single photon [30], or exchange its position with a single photon [29,31].

In this Letter, we establish a different type of atom-photon interaction in the Rydberg EIT system, with which a single photon can exchange its spin state with a single atom. It is achieved by coupling photons to an atomic ensemble that interacts with a single control atom via Rydberg dressing [32,33]. We show that under suitable conditions, the scattering dynamics can be tuned from dissipative to coherent. In the dissipative regime, the system evolves robustly into an entangled dark state of a photon and the control atom. For coherent scattering, the dynamics maps to a model of generic single-photon subtraction, whose solution reveals a universal trade-off between efficiency and purity of the subtracted single photon, and yields a phase-matching condition for optimizing its performance.

The system we study is illustrated in Fig. 1(a), where the input photon carries photonic spin (polarization) and can exchange its state with the pseudospin (internal state) of the control atom (subscripts a and p refer to atom and photon, respectively). This atom-photon spin-exchange interaction is mediated by an atomic ensemble, which strongly interacts with both the photon and the control atom [34–36]. The level structure shown in Fig. 1(b) helps to realize such an interaction. A photon propagates in an

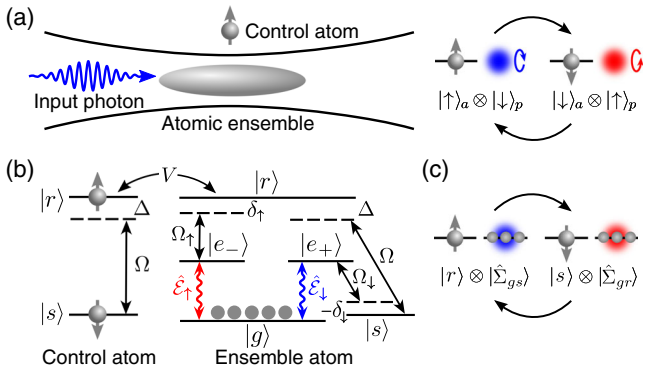

FIG. 1. (a) Schematic for the spin-exchange collision between input photons and the control atom. (b) Level structure for the control atom and the ensemble atom. For ^{87}Rb atom, we can choose $|g\rangle = |5S_{1/2}, F = 1, m_F = 0\rangle$, $|e_\pm\rangle = |5P_{3/2}, F = 2, m_F = \pm 1\rangle$, $|s\rangle = |5S_{1/2}, F = 2, m_F = 0\rangle$, and $|r\rangle = |nS_{1/2}, J = 1/2, m_J = -1/2\rangle$. The coupling Ω between $|s\rangle$ and $|r\rangle$ can be constructed using a two-photon process with an intermediate state $|5P_{1/2}, F = 1, m_F = -1\rangle$. The two-photon detunings are $\delta_\downarrow = \Omega^2/\Delta$ and $\delta_\uparrow = -\delta_\downarrow$ to compensate for dressing induced level shifts of states $|r\rangle$ and $|s\rangle$. (c) Schematic of the spin exchange between the control atom and a spin-wave excitation in the ensemble.

atomic ensemble via two distinct EIT processes [37,38]: the left circularly polarized (pseudo-spin-up) photonic field $\hat{\mathcal{E}}_\uparrow(\mathbf{r})$ forms a Rydberg EIT involving the ground state $|g\rangle$, the intermediate state $|e_-\rangle$, and the Rydberg state $|r\rangle$; while the right circularly polarized (pseudo-spin-down) photonic field $\hat{\mathcal{E}}_\downarrow(\mathbf{r})$ participates in a Λ-type EIT formed by $|g\rangle$, $|e_+\rangle$, and another ground state $|s\rangle$. In addition, state $|s\rangle$ is dressed to Rydberg state $|r\rangle$ for both the control atom and ensemble atoms.

It is shown in Ref. [33] that the above dressing scheme induces an effective spin-exchange interaction $\hat{V}_{\rm ex}$ between atoms in $|s\rangle$ and $|r\rangle$. At low photon density, interactions between ensemble atoms are negligible, such that $\hat{V}_{\rm ex}=\sum_i U(\mathbf{r}_i)\hat{\sigma}_{rs}\hat{\sigma}^i_{sr}+\text{H.c.}$ just describes the spin-exchange between the control atom ($\hat{\sigma}_{\mu\nu}=|\mu\rangle\langle\nu|$) and each ith atom in the ensemble ($\hat{\sigma}^i_{\mu\nu}$). Since most ensemble atoms are in the ground state $|g\rangle$, $\hat{V}_{\rm ex}$ actually describes the spin-exchange between the control atom and a collective excitation (spin-wave) in the atomic ensemble [Fig. 1(c)], i.e., $\hat{V}_{\rm ex}=\int d\mathbf{r}U(\mathbf{r})\hat{\sigma}_{rs}\hat{\Sigma}^\dagger_{gs}(\mathbf{r})\hat{\Sigma}_{gr}(\mathbf{r})+\text{H.c.}$, where $\hat{\Sigma}_{g\mu}(\mathbf{r})$ denotes the spin-wave field operator for the collective excitation in state $|\mu\rangle$ [39]. With the above EIT configuration, the spin-wave field $\hat{\Sigma}_{gr}(\mathbf{r})$ is coupled to the photonic field $\hat{\mathcal{E}}_\uparrow(\mathbf{r})$ to form a dark state polariton (DSP) field [41] $\hat{\Psi}_\uparrow(\mathbf{r})=\hat{\mathcal{E}}_\uparrow(\mathbf{r})\cos\theta_\uparrow-\hat{\Sigma}_{gr}(\mathbf{r})\sin\theta_\uparrow$, while $\hat{\Sigma}_{gs}(\mathbf{r})$ is coupled to $\hat{\mathcal{E}}_\downarrow(\mathbf{r})$ to form another DSP $\hat{\Psi}_\downarrow(\mathbf{r})=\hat{\mathcal{E}}_\downarrow(\mathbf{r})\cos\theta_\downarrow-\hat{\Sigma}_{gs}(\mathbf{r})\sin\theta_\downarrow$, with $\tan\theta_\mu=g_p/\Omega_\mu$. In this way, $\hat{V}_{\rm ex}$ maps to the exchange interaction between the control atom and the photonic field.

The exchange interaction takes the form $U(\mathbf{r})=U_0/[1+(|\mathbf{r}|/R_c)^6]$, where the strength $U_0=\Omega^2/\Delta$ is determined by the Rabi frequency Ω and the detuning Δ of the dressing field ($\Omega\ll\Delta$), and the effective range is $R_c=(C_6/\Delta)^{1/6}$ with C_6 the van der Waals (vdW) interaction coefficient between atoms in state $|r\rangle$ [33]. It does not need one to tune near a Föster resonance and can be conveniently controlled by the dressing field. Furthermore, the dressing scheme adopted here suppresses the unwanted direct interaction ($\sim\Omega^4/\Delta^3$) between input photons in mode $\hat{\mathcal{E}}_\downarrow$. These desirable features as well as other details are compared to the off-diagonal vdW interaction scheme in the Supplemental Material [39].

Single-photon scattering.—First, we consider the interaction between the control atom and a single photon propagating along z direction. Neglecting the decoherence of the Rydberg state, the input or output state in the one-dimensional (1D) case can be expressed as

$$|\psi(t)\rangle=\int dz E_{\downarrow\uparrow}(z,t)\hat{\mathcal{E}}^\dagger_\downarrow(z)|0\rangle\otimes|\uparrow\rangle_a+\int dz E_{\uparrow\downarrow}(z,t)\hat{\mathcal{E}}^\dagger_\uparrow(z)|0\rangle\otimes|\downarrow\rangle_a, \quad (1)$$

where $|0\rangle$ denotes the vacuum state for photons, and $|\uparrow\rangle_a=|r\rangle$, $|\downarrow\rangle_a=|s\rangle$ represent two internal states of the control atom. The spatiotemporal feature of the photon is described by the wave function $E_{\mu\nu}(z,t)=\langle\nu|_a\langle 0|\hat{\mathcal{E}}_\mu(z)|\psi(t)\rangle$. The output state of the system is determined by the dynamics inside the atomic ensemble $z\in[0,L]$, where the spin-wave field needs to be taken into consideration. Let $P_{\downarrow\uparrow}$, $S_{\downarrow\uparrow}$, $P_{\uparrow\downarrow}$, and $S_{\uparrow\downarrow}$ describe the collective excitation in state $|e_+\rangle$, $|s\rangle$, $|e_-\rangle$, and $|r\rangle$, respectively [42]. Then the evolution of the wave function $\psi(z,t)=(E_{\downarrow\uparrow},P_{\downarrow\uparrow},S_{\downarrow\uparrow},E_{\uparrow\downarrow},P_{\uparrow\downarrow},S_{\uparrow\downarrow})^T$ is governed by $i\partial_t\psi=\mathcal{H}\psi$ [39] with

$$\mathcal{H}=\begin{bmatrix}-ic\partial_z & g_p & 0 & 0 & 0 & 0\\ g_p & -i\gamma & \Omega_\downarrow & 0 & 0 & 0\\ 0 & \Omega_\downarrow & U(z) & 0 & 0 & U(z)\\ 0 & 0 & 0 & -ic\partial_z & g_p & 0\\ 0 & 0 & 0 & g_p & -i\gamma & \Omega_\uparrow\\ 0 & 0 & U(z) & 0 & \Omega_\uparrow & U(z)\end{bmatrix}, \quad (2)$$

where g_p and 2γ are the collective atom-photon coupling constant and the linewidth of the $|g\rangle-|e_\pm\rangle$ transition, respectively, $\Omega_\uparrow$ ($\Omega_\downarrow$) denotes the control field for the Rydberg (Λ-type) EIT, and $U(z)=U_0/[1+(\sqrt{z^2+r_\perp^2}/R_c)^6]$ is the potential. In the frequency (ω) domain, we have

$$i\partial_z\begin{bmatrix}E_{\downarrow\uparrow}\\ E_{\uparrow\downarrow}\end{bmatrix}=\begin{bmatrix}\chi_\downarrow(z,\omega) & \kappa(z,\omega)\\ \kappa(z,\omega) & \chi_\uparrow(z,\omega)\end{bmatrix}\begin{bmatrix}E_{\downarrow\uparrow}\\ E_{\uparrow\downarrow}\end{bmatrix}, \quad (3)$$

where the susceptibilities $\chi_\downarrow$ and $\chi_\uparrow$ come from the dressing induced diagonal interaction, while κ describes the spin-exchange coupling between states $|\downarrow\rangle_p\otimes|\uparrow\rangle_a$ and $|\uparrow\rangle_p\otimes|\downarrow\rangle_a$. For the input state $|\downarrow\rangle_p\otimes|\uparrow\rangle_a$, the solution to Eq. (3) can be written as $E_{\downarrow\uparrow}(L,\omega)=T(\omega)E_{\downarrow\uparrow}(0,\omega)$, and $E_{\uparrow\downarrow}(L,\omega)=R(\omega)E_{\downarrow\uparrow}(0,\omega)$. At steady state ($\omega=0$), we find $\chi_\mu(z,0)=\mathcal{V}(z)/v_\mu$, and $\kappa(z,0)=\mathcal{V}(z)/\sqrt{v_\uparrow v_\downarrow}$, where $v_\mu=c\Omega_\mu^2/g_p^2$ ($\mu=\uparrow,\downarrow$) is the photon group velocity in the slow-light regime, and

$$\mathcal{V}(z)=\frac{U(z)}{1+i\gamma U(z)(\Omega_\downarrow^2+\Omega_\uparrow^2)/\Omega_\downarrow^2\Omega_\uparrow^2} \quad (4)$$

is the effective potential. In this case, the scattering coefficients $T(0)=(\Omega_\uparrow^2e^{-i2\phi}+\Omega_\downarrow^2)/(\Omega_\downarrow^2+\Omega_\uparrow^2)$ and $R(0)=\Omega_\uparrow\Omega_\downarrow(e^{-i2\phi}-1)/(\Omega_\downarrow^2+\Omega_\uparrow^2)$ are determined by the interaction induced phase factor $\phi=(v_\uparrow+v_\downarrow)\int_0^L dz\mathcal{V}(z)/2v_\uparrow v_\downarrow$. For $L>4R_c$ and $r_\perp<R_c$, the complex phase factor is simply given by $\phi\approx(2\pi/3)\xi[1-i(5/3)\xi]\times\text{OD}_c$, where $\xi=U_0/\gamma_{\rm EIT}$ measures the interaction strength in

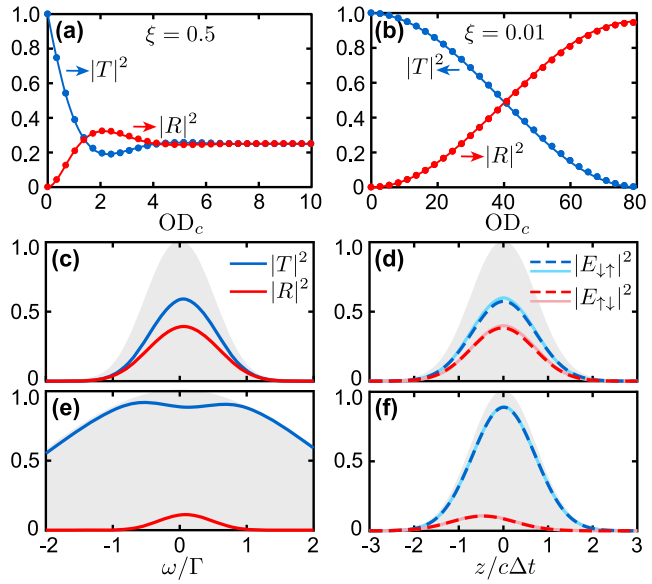

FIG. 2. (a),(b) Scattering coefficients versus OD_c in the dissipative ($\xi = 0.5$) and the coherent ($\xi = 0.01$) regime. The dots and the solid lines correspond to the results for a Gaussian beam with a waist w and the 1D model, respectively. We take $\Omega_{\uparrow,\downarrow}/2\pi = 3$ MHz and $R_c = 9$ μm in (a), $\Omega_{\uparrow,\downarrow}/2\pi = 8$ MHz and $R_c = 12$ μm in (b), $\gamma/2\pi = 3$ MHz, $r_\perp = 2w = 4$ μm, $L = 4R_c$, and $\Delta = 10$ Ω. (c)–(f) Spectra of the scattering coefficients in units of the EIT bandwidth $\Gamma = \Omega_\uparrow^2/\gamma\sqrt{\mathrm{OD}}$ [$\mathrm{OD} = (L/R_c)\mathrm{OD}_c$] and evolution of the wave functions for a Gaussian input pulse with a duration $\Delta t = 10/\Gamma$. The shaded areas denote the noninteracting transmission. The dashed and the solid lines in (d) and (f) are based on Eqs. (3) and (5), respectively. The parameters are the same as in (b) ($\mathrm{OD}_c = 35$) except that we introduce a group velocity mismatch in (e) and (f) by taking $\Omega_\downarrow/2\pi = 16$ MHz.

units of the effective EIT linewidth $\gamma_{\mathrm{EIT}} = 2\Omega_\uparrow^2\Omega_\downarrow^2/(\Omega_\downarrow^2 + \Omega_\uparrow^2)\gamma$, and $\mathrm{OD}_c = g_p^2 R_c/\gamma c$ denotes the effective optical depth.

When the interaction strength U_0 is comparable to the EIT linewidth $\Omega_\uparrow^2/\gamma$ or $\Omega_\downarrow^2/\gamma$, the ratio ξ is large. Consequently, both $\mathcal{V}(z)$ and ϕ have a large imaginary part. In this dissipative interacting regime, as OD_c increases, the photon loss probability rapidly grows. However, Eq. (3) possesses an eigenstate free from dissipation, such that as OD_c increases further, the loss rate saturates, and the system eventually evolves into this dark state $(\Omega_\downarrow|\downarrow\rangle_p|\uparrow\rangle_a - \Omega_\uparrow|\uparrow\rangle_p|\downarrow\rangle_a)/(\Omega_\downarrow^2 + \Omega_\uparrow^2)^{1/2}$ with a probability $\Omega_\downarrow^2/(\Omega_\downarrow^2 + \Omega_\uparrow^2)$ [Fig. 2(a)]. Thus, such a dissipative spin-exchange collision can be used for robust generation of atom-photon entanglement. If the interaction strength is much smaller than the EIT linewidth, i.e., $\xi \ll 1$, the effective potential $\mathcal{V}(z) \approx U(z)$ is essentially real and the imaginary part of ϕ is largely suppressed. In this case, as OD_c increases, the system undergoes a coherent oscillation between $|\downarrow\rangle_p \otimes |\uparrow\rangle_a$ and $|\uparrow\rangle_p \otimes |\downarrow\rangle_a$ [Fig. 2(b)]. We calculate the scattering coefficients for a finite beam width $w < R_c$ [31] [see Figs. 2(a) and 2(b)], and find nice agreement with the results predicted by the 1D model.

The single-photon scattering elucidated above can be used as a building block in quantum networks. For scattering at small OD_c, whether dissipative or coherent, the induced atom-photon entanglement can be purified to establish quality entanglement between distant atoms [39]. Unlike the DLCZ protocol [43], the entanglement we discuss here refers to polarization bases instead of Fock space, so that photon-number resolved detectors are not required, and the system is insensitive to interferometric instabilities [8,44]. At large OD_c, it is possible to make $\phi = \pi/2$ at $\Omega_\uparrow = \Omega_\downarrow$, such that the collision leads to a coherent mapping between atomic and photonic states, i.e., $|\downarrow\rangle_p \otimes (\alpha|\downarrow\rangle + \beta|\uparrow\rangle)_a \leftrightarrow (\alpha|\downarrow\rangle - \beta|\uparrow\rangle)_p \otimes |\downarrow\rangle_a$, which facilitates quantum state transfer in a network.

We now focus on the coherent scattering process where dissipation is negligible. In this case, the light propagation inside the atomic ensemble can be described by DSP fields $\hat{\Psi}_\uparrow(z)$ and $\hat{\Psi}_\downarrow(z)$. For frequency components well within the EIT bandwidth, the dynamics of DSP fields are governed by the Hamiltonian

$$\begin{aligned}\hat{H} = &-iv_\downarrow \int dz\hat{\Psi}_\downarrow^\dagger(z)\partial_z\hat{\Psi}_\downarrow(z) - iv_\uparrow \int dz\hat{\Psi}_\uparrow^\dagger(z)\partial_z\hat{\Psi}_\uparrow(z)\\ &+ \int dzU(z)[\hat{\sigma}_{\uparrow\uparrow}\hat{\Psi}_\downarrow^\dagger(z)\hat{\Psi}_\downarrow(z) + \hat{\sigma}_{\downarrow\downarrow}\hat{\Psi}_\uparrow^\dagger(z)\hat{\Psi}_\uparrow(z)]\\ &+ \int dzU(z)[\hat{\sigma}_{\uparrow\downarrow}\hat{\Psi}_\downarrow^\dagger(z)\hat{\Psi}_\uparrow(z) + \mathrm{H.c.}], \qquad (5)\end{aligned}$$

whose first line denotes the photon kinetic energy, and the second (third) line represents the density (spin-exchange) interaction between the photon and the atom. As shown in Figs. 2(c)–2(f), this Hamiltonian is accurate for describing coherent scatterings [the asymmetries between different components in Figs. 2(e) and 2(f) arise from the mismatch of velocities $v_\uparrow$ and $v_\downarrow$].

Multiphoton scattering.—Next, we consider coherent spin-exchange collisions between the control atom and an input pulse containing n identical photons. Here, we focus on the limit of a long input pulse with a duration $\Delta t \gg nR_c/v_\mu$. In this low-photon-density regime, photons rarely interact with the control atom at the same time, which allows us to obtain an analytical form for the output state based on single-photon scattering coefficients, without numerically solving the multiphoton Schrödinger equation based on Eq. (5).

Assuming the n incoming photons are in the spin-down state with a real temporal wave function $h(t)$ normalized as $\int dth^2(t) = 1$ and the control atom is initially spin-up, the input state of the system is given by (taking $c = 1$)

$$|\psi_{\rm in}(t)\rangle = \frac{1}{\sqrt{n!}}\left[\int_{-\infty}^{\infty} dz h(t-z)\hat{\mathcal{E}}_{\downarrow}^{\dagger}(z)\right]^{n}|0\rangle|\uparrow\rangle_a,$$
$$= \sqrt{n!}\int_{t_n>\cdots>t_1}\left[\prod_{i=1}^{n} dt_i h(t_i)\hat{\mathcal{E}}_{\downarrow}^{\dagger}(t-t_i)\right]|0\rangle|\uparrow\rangle_a,$$

where time ordering for the input photons is introduced [45]. For coherent spin-exchange collisions governed by Eq. (5), the total magnetization $\hat{\sigma}_{\uparrow\uparrow} + \int dz\hat{\Psi}_{\uparrow}^{\dagger}(z)\hat{\Psi}_{\uparrow}(z) = 1$ is conserved, which implies that at most one of the photons can be scattered to flip its spin state. At low photon density, photons interact with the atom one after the other; i.e., if a photon propagates through the medium without exchanging its state with the atom, the next photon still has a probability to do so; but once the exchange occurs, the remaining photons will keep their spin states. In this way, the output state is given by

$$|\psi(t)\rangle = T^n|\psi_{\rm in}(t-\tau)\rangle + \sqrt{n!}\sum_{m=1}^{n} RT^{m-1}|\psi_m(t)\rangle, \quad (6)$$

where $|\psi_{\rm in}(t-\tau)\rangle$ corresponds to the situation in which no spin-exchange occurs, while $|\psi_m(t)\rangle$ denotes the event that the spin-exchange is between the control atom and the mth photon in the pulse, given by

$$|\psi_m(t)\rangle = \int_{t_n>\cdots>t_{m+1}}\left[\prod_{i=m+1}^{n} dt_i h(t_i)\hat{\mathcal{E}}_{\downarrow}^{\dagger}(t-\tau'-t_i)\right]$$
$$\times\int_{-\infty}^{t_{m+1}} dt_m h(t_m)\hat{\mathcal{E}}_{\uparrow}^{\dagger}(t-\tau-t_m)$$
$$\times\int_{t_m>\cdots>t_1}\left[\prod_{i=1}^{m-1} dt_i h(t_i)\hat{\mathcal{E}}_{\downarrow}^{\dagger}(t-\tau'-t_i)\right]|0\rangle|\downarrow\rangle_a,$$

with τ and τ' the EIT-induced delay time [39] for spin-up and spin-down photons, respectively. In fact, the spin-exchange collision here can be viewed as a heralded single-photon subtractor: a single photon is subtracted from mode $\hat{\mathcal{E}}_{\downarrow}$ and added to mode $\hat{\mathcal{E}}_{\uparrow}$, conditioned on the spin-flip of the control atom. In contrast to previous schemes [46,47], the single-photon is coherently extracted from the multi-photon pulse here, so it simultaneously behaves as a single-photon source [48,49].

Since the extracted single-photon and the remaining $n-1$ spin-down photons together constitute a pure state, the performance of such a single-photon subtractor can be measured by either part of the system. Tracing out $n-1$ photons in mode $\hat{\mathcal{E}}_{\downarrow}$, the reduced density matrix operator for the spin-up single-photon is $\hat{\rho} = \int dxdy\rho(x,y)\times\hat{\mathcal{E}}_{\uparrow}^{\dagger}(x)|0\rangle\langle 0|\hat{\mathcal{E}}_{\uparrow}(y)$, with the density matrix element $\rho(x,y) = \tilde{\rho}(t-\tau-x, t-\tau-y)$ and [50]

$$\tilde{\rho}(x,y) = n|R|^2 h(x)h(y)\left[|T|^2\int_{-\infty}^{\min(x,y)} dz h^2(z) + T\int_{\min(x,y)}^{\max(x,y)} dz h^2(z) + \int_{\max(x,y)}^{+\infty} dz h^2(z)\right]^{n-1}. \quad (7)$$

The efficiency for scattering a single photon to spin-up state is found to be $\eta = {\rm tr}[\hat{\rho}] = 1-|T|^{2n}$, and the purity of this extracted single-photon is given by $\mathcal{P} = {\rm tr}[\hat{\rho}^2]/{\rm tr}[\hat{\rho}]^2$, which has an analytical expression

$$\mathcal{P} = \frac{n(1+T)(1-T^{2n-1})}{(2n-1)(1-T^{2n})}, \quad (8)$$

if $T = \sqrt{1-|R|^2}e^{i\theta}$ is real (i.e., $\theta = 0, \pi$). For $\theta = 0$, this result proves the fundamental trade-off between efficiency and purity of the single-photon subtraction observed in Ref. [24]: while the decrease of the single-photon exchange rate $|R|^2$ reduces the efficiency η, it yields a larger single-photon purity $\mathcal{P}$. The physical origin of this trade-off comes from entanglement between the subtracted single-photon and the remaining $n-1$ photons. For a perfect exchange $|R| = 1$, only $|\psi_1\rangle$ survives in Eq. (6), so the timing for the first photon in mode $\hat{\mathcal{E}}_{\downarrow}$ carries correlated information about the photon in mode $\hat{\mathcal{E}}_{\uparrow}$. This entanglement results in an impure spin-up photon with $\mathcal{P} = n/(2n-1)$, exactly the case discussed in Ref. [45]. In contrast, for $|R| \ll 1$ ($T \approx 1$), each $|\psi_m\rangle$ in Eq. (6) is almost equally weighted, so the timing of the spin-up photon is uncorrelated with the timings of the $n-1$ spin-down photons, i.e., they are not entangled. Therefore, the subtracted photon is almost pure with $\tilde{\rho}(x,y) \sim h(x)h(y)$ and $\mathcal{P} \approx 1$. To verify the above analysis, we perform numerical simulations for $n = 2$ based on Eq. (5). As shown in Fig. 3, the existence of this trade-off is largely confirmed and good agreement with analytical predictions is observed.

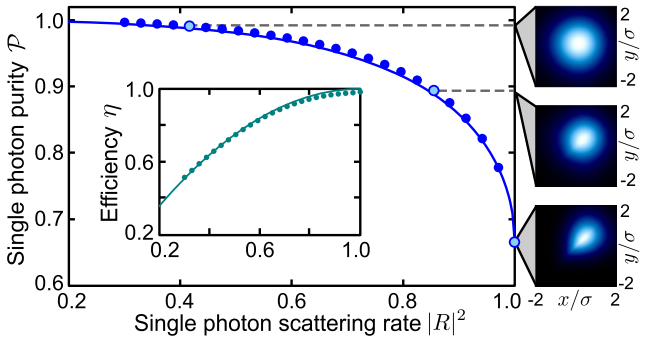

FIG. 3. Purity and efficiency of the extracted photon. The dots and the solid lines represent numerical ($v_{\downarrow}\Delta t = 20R_c$) and analytical results, respectively. The right figures show the normalized density matrix $|\rho(x,y)|/\eta$ (brighter colors indicate larger values). To assure $\theta = 0$, we set $\phi = \pi/2$ and $\Omega_{\downarrow} > \Omega_{\uparrow}$.

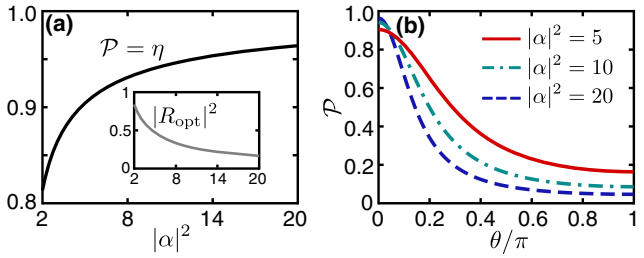

FIG. 4. (a) Optimized purity and efficiency for the scattering of a coherent input with mean photon number $|\alpha|^2$ ($\theta=0$). The inset shows the optimal scattering rate $|R_{\rm opt}|^2$. (b) Purity $\mathcal{P}$ as a function of the phase θ of the scattering coefficient T at $|R_{\rm opt}|^2$ for the indicated value of $|\alpha|^2$.

The above analysis is universal for a wide class of single photon subtractors in the literature [24,46–49], where identical photons interact with the local system sequentially: once the system changes the state of a photon, its own state is changed as well and all subsequent photons are protected from being scattered. As a result, the order of arrival for the incoming identical photons determines the output state. Although the universal trade-off in this type of device prevents the implementation of a perfect single-photon subtraction with $\eta=\mathcal{P}=1$ for arbitrary incoming states, it remains possible to achieve high efficiency and purity simultaneously for a large input photon number. To demonstrate this, we consider the scattering of a coherent input state $e^{-|\alpha|^2/2}\sum_n(\alpha^n/\sqrt{n!})|n\rangle$ with an optimal scattering rate $|R_{\rm opt}|^2$ that gives $\eta=\mathcal{P}$. With such an optimization, both purity and efficiency approach unity [shown in Fig. 4(a), $\mathcal{P}=\eta\approx 1-(\ln|\alpha|^2)/4|\alpha|^2$ for $|\alpha|^2\gg 1$] as the mean photon number $|\alpha|^2$ increases, which improves on the $|R|=1$ case discussed in Ref. [45] ($\eta=1,\mathcal{P}=0.5$; or $\eta=0.69$, $\mathcal{P}=1$ after purification).

Finally, we emphasize that to achieve the optimal purity, the phase of $T=|T|e^{i\theta}$ needs to be zero; i.e., photons remaining in mode $\hat{\mathcal{E}}_\downarrow$ should acquire the same phase irrespective of whether the spin exchange happens or not. The monotonic decrease of purity [$\mathcal{P}\approx(1-|T|^2)/2(1-|T|\cos\theta)$ for $|\alpha|^2\gg 1$] with the phase mismatch θ [Fig. 4(b)] can be understood as follows: the phase $(m-1)\theta$ imprinted on $|\psi_m\rangle$ in Eq. (6) causes the phase distribution of the spin-up photon strongly correlated with the timing of the remaining photons. In the limit of $|T|\approx 1$ and $\theta=\pi$, the purity $\mathcal{P}\approx 1/(2n-1)$ is even worse than a perfect exchange, although the probability distribution $\tilde{\rho}(x,x)\sim h^2(x)$ remains unaltered. Such a phase-matching condition highlights the coherent feature of the single-photon subtraction, which cannot be captured by the Monte Carlo simulation used in Ref. [24].

In conclusion, we present a scheme to engineer spin-exchange interactions between photons and a single atom, and discuss the scattering dynamics for a single-photon as well as a multiphoton input. Further studies can use some recently developed techniques [51–54] to address the interesting multiphoton scattering problem beyond the low-photon-density regime, where collective effects will come into play. The system can also be used to perform quantum logic operations, such as single-photon optical switching [55]. Besides facilitating quantum information processing, the spin-exchange collision discussed here opens a new avenue for the study of strong light-atom interactions.

We acknowledge valuable discussions with Cheng Chen, Alexey Gorshkov, Ron Belyansky, and Lin Li. This work is supported by the National Key R&D Program of China (Grant No. 2018YFA0306504) and the National Natural Science Foundation of China (NSFC) (Grants No. 11654001, No. U1930201, No. 91736106, No. 11674390, No. 91836302 and No. 91736311). L. Y. also acknowledges support from Beijing Academy of Quantum Information Sciences (BAQIS) Research Program (Grant No. Y18G24).

*ycliu@tsinghua.edu.cn
†lyou@mail.tsinghua.edu.cn

[1] J. I. Cirac and H. J. Kimble, Nat. Photonics **11**, 18 (2017).
[2] G. Rempe, H. Walther, and N. Klein, Phys. Rev. Lett. **58**, 353 (1987).
[3] Y. Zhu, D. J. Gauthier, S. E. Morin, Q. Wu, H. J. Carmichael, and T. W. Mossberg, Phys. Rev. Lett. **64**, 2499 (1990).
[4] R. J. Thompson, G. Rempe, and H. J. Kimble, Phys. Rev. Lett. **68**, 1132 (1992).
[5] M. Brune, F. Schmidt-Kaler, A. Maali, J. Dreyer, E. Hagley, J. M. Raimond, and S. Haroche, Phys. Rev. Lett. **76**, 1800 (1996).
[6] J. M. Raimond, M. Brune, and S. Haroche, Rev. Mod. Phys. **73**, 565 (2001).
[7] H. Kimble, Nature (London) **453**, 1023 (2008).
[8] N. Sangouard, C. Simon, H. de Riedmatten, and N. Gisin, Rev. Mod. Phys. **83**, 33 (2011).
[9] A. Reiserer and G. Rempe, Rev. Mod. Phys. **87**, 1379 (2015).
[10] A. González-Tudela, C.-L. Hung, D. E. Chang, J. I. Cirac, and H. Kimble, Nat. Photonics **9**, 320 (2015).
[11] J. S. Douglas, H. Habibian, C.-L. Hung, A. V. Gorshkov, H. J. Kimble, and D. E. Chang, Nat. Photonics **9**, 326 (2015).
[12] C.-L. Hung, A. González-Tudela, J. I. Cirac, and H. Kimble, Proc. Natl. Acad. Sci. U.S.A. **113**, E4946 (2016).
[13] D. E. Chang, J. S. Douglas, A. González-Tudela, C.-L. Hung, and H. J. Kimble, Rev. Mod. Phys. **90**, 031002 (2018).
[14] F. Haas, J. Volz, R. Gehr, J. Reichel, and J. Estève, Science **344**, 180 (2014).
[15] R. McConnell, H. Zhang, J. Hu, S. Ćuk, and V. Vuletić, Nature (London) **519**, 439 (2015).
[16] S. J. Masson, M. D. Barrett, and S. Parkins, Phys. Rev. Lett. **119**, 213601 (2017).

[17] M. Saffman, T. G. Walker, and K. Mølmer, Rev. Mod. Phys. **82**, 2313 (2010).

[18] M. Fleischhauer, A. Imamoglu, and J. P. Marangos, Rev. Mod. Phys. **77**, 633 (2005).

[19] J. D. Pritchard, D. Maxwell, A. Gauguet, K. J. Weatherill, M. P. A. Jones, and C. S. Adams, Phys. Rev. Lett. **105**, 193603 (2010).

[20] A. V. Gorshkov, J. Otterbach, M. Fleischhauer, T. Pohl, and M. D. Lukin, Phys. Rev. Lett. **107**, 133602 (2011).

[21] T. Peyronel, O. Firstenberg, Q.-Y. Liang, S. Hofferberth, A. V. Gorshkov, T. Pohl, M. D. Lukin, and V. Vuletic, Nature (London) **488**, 57 (2012).

[22] S. Baur, D. Tiarks, G. Rempe, and S. Dürr, Phys. Rev. Lett. **112**, 073901 (2014).

[23] H. Gorniaczyk, C. Tresp, J. Schmidt, H. Fedder, and S. Hofferberth, Phys. Rev. Lett. **113**, 053601 (2014).

[24] C. Tresp, C. Zimmer, I. Mirgorodskiy, H. Gorniaczyk, A. Paris-Mandoki, and S. Hofferberth, Phys. Rev. Lett. **117**, 223001 (2016).

[25] V. Parigi, E. Bimbard, J. Stanojevic, A. J. Hilliard, F. Nogrette, R. Tualle-Brouri, A. Ourjoumtsev, and P. Grangier, Phys. Rev. Lett. **109**, 233602 (2012).

[26] D. Tiarks, S. Schmidt, G. Rempe, and S. Dürr, Sci. Adv. **2**, e1600036 (2016).

[27] D. Tiarks, S. Schmidt, T. Stolz, G. Rempe, and S. Dürr, Nat. Phys. **15**, 124 (2019).

[28] O. Firstenberg, C. S. Adams, and S. Hofferberth, J. Phys. B **49**, 152003 (2016).

[29] J. D. Thompson, T. L. Nicholson, Q.-Y. Liang, S. H. Cantu, A. V. Venkatramani, S. Choi, I. A. Fedorov, D. Viscor, T. Pohl, M. D. Lukin *et al.*, Nature (London) **542**, 206 (2017).

[30] C. R. Murray and T. Pohl, Phys. Rev. X **7**, 031007 (2017).

[31] M. Khazali, C. R. Murray, and T. Pohl, Phys. Rev. Lett. **123**, 113605 (2019).

[32] A. W. Glaetzle, K. Ender, D. S. Wild, S. Choi, H. Pichler, M. D. Lukin, and P. Zoller, Phys. Rev. X **7**, 031049 (2017).

[33] F. Yang, S. Yang, and L. You, Phys. Rev. Lett. **123**, 063001 (2019).

[34] M. Saffman and T. G. Walker, Phys. Rev. A **72**, 042302 (2005).

[35] D. Petrosyan and K. Mølmer, Phys. Rev. Lett. **121**, 123605 (2018).

[36] A. Grankin, P. O. Guimond, D. V. Vasilyev, B. Vermersch, and P. Zoller, Phys. Rev. A **98**, 043825 (2018).

[37] J. Ruseckas, V. Kudriašov, A. Mekys, T. Andrijauskas, I. A. Yu, and G. Juzeliūnas, Phys. Rev. A **98**, 013846 (2018).

[38] F. Yang, Y.-C. Liu, and L. You, Phys. Rev. A **99**, 063803 (2019).

[39] See the Supplemental Material at http://link.aps.org/supplemental/10.1103/PhysRevLett.125.143601 for more details on the calculations and experimental considerations, which includes Ref. [40].

[40] J. Li, M.-T. Zhou, C.-W. Yang, P.-F. Sun, J.-L. Liu, X.-H. Bao, and J.-W. Pan, Phys. Rev. Lett. **123**, 140504 (2019).

[41] M. Fleischhauer and M. D. Lukin, Phys. Rev. Lett. **84**, 5094 (2000).

[42] The explicit definitions of these excitation wave functions are $P_{\downarrow\uparrow}(z,t) = \langle\uparrow|_a\langle 0|\hat{\Sigma}_{ge_+}(z)|\psi(t)\rangle$, $S_{\downarrow\uparrow}(z,t) = \langle\uparrow|_a\langle 0|\hat{\Sigma}_{gs}(z)|\psi(t)\rangle$, $P_{\uparrow\downarrow}(z,t) = \langle\downarrow|_a\langle 0|\hat{\Sigma}_{ge_-}(z)|\psi(t)\rangle$, and $S_{\uparrow\downarrow}(z,t) = \langle\downarrow|_a\langle 0|\hat{\Sigma}_{gr}(z)|\psi(t)\rangle$.

[43] L.-M. Duan, M. Lukin, J. I. Cirac, and P. Zoller, Nature (London) **414**, 413 (2001).

[44] Z.-B. Chen, B. Zhao, Y.-A. Chen, J. Schmiedmayer, and J.-W. Pan, Phys. Rev. A **76**, 022329 (2007).

[45] A. V. Gorshkov, R. Nath, and T. Pohl, Phys. Rev. Lett. **110**, 153601 (2013).

[46] J. Honer, R. Löw, H. Weimer, T. Pfau, and H. P. Büchler, Phys. Rev. Lett. **107**, 093601 (2011).

[47] C. R. Murray, I. Mirgorodskiy, C. Tresp, C. Braun, A. Paris-Mandoki, A. V. Gorshkov, S. Hofferberth, and T. Pohl, Phys. Rev. Lett. **120**, 113601 (2018).

[48] S. Rosenblum, S. Parkins, and B. Dayan, Phys. Rev. A **84**, 033854 (2011).

[49] S. Rosenblum, O. Bechler, I. Shomroni, Y. Lovsky, G. Guendelman, and B. Dayan, Nat. Photonics **10**, 19 (2016).

[50] Here we assume that the scattering coefficient T is real. For a more general case where T is a complex number, $\tilde{\rho}(x,y)$ is given by Eq. (7) in regions $x \geq y$, and is modified by replacing T with T^* for $x \leq y$.

[51] M. T. Manzoni, D. E. Chang, and J. S. Douglas, Nat. Commun. **8**, 1743 (2017).

[52] E. Zeuthen, M. J. Gullans, M. F. Maghrebi, and A. V. Gorshkov, Phys. Rev. Lett. **119**, 043602 (2017).

[53] P. Bienias, J. Douglas, A. Paris-Mandoki, P. Titum, I. Mirgorodskiy, C. Tresp, E. Zeuthen, M. J. Gullans, M. Manzoni, S. Hofferberth *et al.*, Phys. Rev. Research **2**, 033049 (2020).

[54] A. H. Kiilerich and K. Mølmer, Phys. Rev. Lett. **123**, 123604 (2019).

[55] I. Shomroni, S. Rosenblum, Y. Lovsky, O. Bechler, G. Guendelman, and B. Dayan, Science **345**, 903 (2014).